Morphology of poly(phenylene sulphide) single crystals grown by a two-stage self-seeding technique

Jerry Sengshiu Chung and Peggy Cebe*

Department of Materials Science and Engineering, Massachusetts Institute of Technology, Cambridge, MA 02139, USA

(Received 11 March 1991; revised 18 April 1991; accepted 19 April 1991)

We have successfully developed a two-stage self-seeding technique to grow poly(phenylene sulphide) (PPS) single crystals from dilute solution, and used these single crystals as model materials to investigate the morphological changes dependent upon the seeding and crystallization conditions. The seeding conditions control the coexistence of different crystal types and determine whether isolated single crystals will be grown. The crystal structure and morphology of PPS single crystals have been investigated by using the wide angle X-ray scattering (WAXS) and transmission electron microscopy techniques including surface decoration by polyethylene. The morphology of the PPS single crystals reveals a highly anisotropic needle-like habit with a very smooth fold surface and very rough growth edges. The aspect ratio of the PPS needle-like single crystals increases as the crystallization temperature and molecular weight increase. Formation of needle-like crystals, lack of sectorization, formation of macroscopically rough growth surfaces, and molecular weight and crystallization temperature dependency of crystal habit suggest a crystal growth model in which the PPS molecules fold parallel to the growth direction during the crystal growth stage from dilute solution.

(Keywords: poly(phenylene sulphide); single crystals; morphology)

INTRODUCTION

Poly(*p*-phenylene sulphide) (PPS) is a semicrystalline engineering thermoplastic polymer with applications as a matrix for carbon- and glass-fibre reinforced composites. As a result of its chemical structure, PPS is one of the polymers most resistant to solvent attack. PPS has a glass transition temperature around 90–105°C, melting point around 270–290°C and degree of crystallinity near 65%[1]. In addition to its excellent mechanical properties, PPS is one of the few polymers which, upon exposure to strong oxidizing agents, becomes electrically conducting[2]. Melt crystallized PPS has been the subject of many recent investigations into its structure[3–6] and crystallization behaviour[7–11]. In 1982, Padden and Lovinger[12] showed that PPS could be successfully dissolved in 1-chloronaphthalene at elevated temperatures. Embryonic spherulites and lenticular crystal aggregates were originally reported[12] and in later work irregular multiple crystalline lamellae giving arc-like diffraction were obtained[13]. Other groups have also reported on solution grown PPS. Uemura *et al.* performed high resolution transmission electron microscopy (TEM) on sheaf-like PPS spherulites and multiple crystalline aggregates[14,15]. D'Ilario and Piozzi studied what were termed single crystals of PPS[16,17] but which appear to be multiple crystalline aggregates.

In this work we report for the first time the dependence of morphology on the conditions of crystallization for solution grown crystals of PPS. Under controlled growth conditions, the first true single crystals have been grown which produce spot-like diffraction and exhibit highly anisotropic growth with needle-like habit. All previous investigators report on solution grown crystals formed using a single-stage method of growth[12–17]. Here we use the two-stage, self-seeding method[18] to grow single crystals of PPS from solution. The two-stage method allows us to control the crystal growth carefully through control of both seeding and growth temperatures. The aspect ratio of PPS single crystals depends strongly upon growth temperature as it does for polyethylene (PE)[19]. Aspect ratios for PPS single crystals can be as high as 20, depending upon molecular weight of the starting material and on the growth temperature. The melting behaviour and X-ray scattering from single crystal mats are also described.

EXPERIMENTAL

Materials

Two grades of powder PPS, Ryton V-1 and experimental film grade, were supplied from Phillips Petroleum Company. The commercial Ryton V-1 is a low molecular weight linear chain PPS ($M_w = \sim 15\,000$) containing low molecular weight oligomers. The experimental film grade is a medium molecular weight grade ($M_w = \sim 60\,000$) of lightly branched PPS with melt index of 49 g per 10 min. Branching is achieved by incorporating trifunctional monomers into the polymer main chain. Both grades of PPS powder were Soxhlet extracted in tetrahydrofuran (THF) for 24 h to remove low molecular weight oligomers.

* To whom correspondence should be addressed

0032-3861/92/081594-12

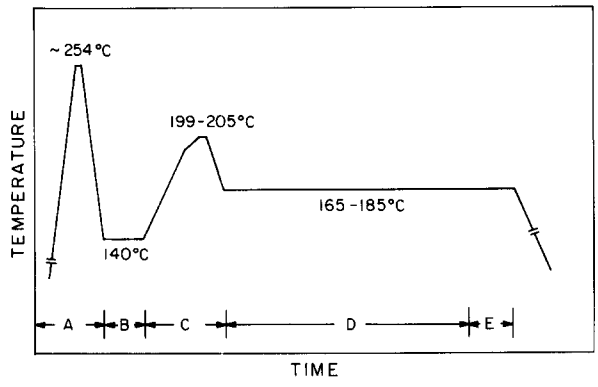

Figure 1 Schematic of the two-stage self-seeding procedure to grow PPS single crystals in dilute 1-chloronaphthalene solution: (A) dissolution stage; (B) first-stage isothermal crystallization; (C) seed generation stage; (D) second-stage isothermal crystallization; (E) solution separation and replacement stage

Two-stage self-seeding method

A two-stage self-seeding method was developed to grow PPS single crystals from dilute solution. The polymer concentration was 0.02 wt% PPS powder in 1-chloronaphthalene solvent. A schematic diagram of the two-stage self-seeding procedure is shown in *Figure 1*. In the dissolution stage, PPS powders were dissolved into one-third the volume of solvent at the reflux temperature (~254°C), then immediately transferred into the crystallization vessel in which two-thirds of the solvent had been preheated at the first-stage crystallization temperature (T_c = 140.0°C for both materials). Imperfect crystals resulted from this first-stage crystallization due to the very fast crystal growth rate. The solution containing suspended crystals was then slowly heated (~20°C h^{-1}) to 5°C below the seeding temperature T_e, then further heated at 2°C h^{-1} to T_e. T_e was chosen to be a few degrees above the temperature at which the solution visibly cleared. At T_e most of the polymer crystal was dissolved, leaving only very small crystals to serve as seed crystals. The T_e was 201°C for Ryton V-1 and 205°C for the film grade PPS.

After the seed crystals were generated, the solution was quickly cooled (~2°C min^{-1}) to a second-stage isothermal T_c. Second-stage crystallization occurred in the temperature range from 165.0 to 185.0°C for both materials for times ranging from 1 to 3 days. After the single crystals formed, they were allowed to precipitate in the crystallization vessel. Then most of the remaining solution containing uncrystallized polymer was removed and fresh solvent was added at the T_c. This procedure was repeated once more to remove most of the uncrystallized polymer fraction which could interfere with further investigations. Since PPS is very sensitive to thermal oxidation[20], the single crystals were grown under argon gas protection from start to end, and only freshly distilled 1-chloronaphthalene solvent was used in order to avoid the presence of dissolved oxygen.

Analysis

Single crystal mats were prepared by slowly filtering the suspended single crystal solution onto a Teflon filter membrane. The mat was blotted between filter papers, then pressed flat and dried in vacuum. D.s.c. studies were performed on a Perkin–Elmer DSC-4 with thermal analysis data station. A scan rate of 10°C min^{-1} was used. Melting temperatures (T_ms) and heats of fusion were calibrated using indium and bismuth standards. Wide angle X-ray scattering (WAXS) experiments were performed on a Rigaku RU-300. National Institute of Standards and Technology silicon powder was used as an internal calibration standard. Since the mat thickness is $\ll$0.1 mm, the position effect of the silicon powder could be neglected. A Jeol JEM-200CX transmission electron microscope was used for morphological studies. The TEM specimens were prepared by depositing single crystal solution on carbon-coated glass slides, floating off on the surface of deionized water, picking up on TEM grids, drying in vacuum, and then shadowing at an angle with gold or gold–palladium alloy.

RESULTS

Effect of seeding temperature

We first investigated the effect of the single-stage isothermal T_c. PPS was dissolved at elevated temperature, and cooled to the first-stage isothermal temperature (140, 150 or 160°C), where the crystals were grown. The morphology of these crystals grown by a single-stage crystallization was always sheaf-like. The morphologies of crystals grown by single-stage crystallization have already been reported[12–17]. Our crystals grown in this manner gave arced diffraction patterns, and are similar in appearance to the multiple crystalline aggregates grown from two-stage growth at too low a T_e. The choice of first-stage isothermal temperature had no effect on the subsequent selection of the T_e for the two-stage growth. We chose 140°C because the completion of the first-stage crystallization took ~4 h, based on visual observation of solution opacity.

The T_e was an important parameter of the two-stage self-seeding procedure. Too low a T_e resulted in formation of sheaf-like multiple crystalline aggregates. *Figures 2* and *3* show aggregates of Ryton V-1 grown at 180.0°C from seeds generated at 199°C (*Figure 2*) and 200°C (*Figure 3*). At the lower T_e (199°C), only multiple crystalline aggregates were seen, while at T_e = 200°C needle-like single crystals are seen to coexist with the sheaf-like structure. The aggregates produced the arced diffraction pattern seen in *Figure 2b* and indexed in the sketch in *Figure 2c*. This arced pattern is entirely typical of all diffraction previously shown for solution grown PPS crystals[12–17]. Using the unit cell parameters of Tabor *et al.*[3] the pattern was indexed as shown, with the *b*-axis aligned parallel to the long direction of the sheaf. This result is similar to that reported by Uemura *et al.*[14,15] and Padden and Lovinger[12] both groups having grown PPS crystals from solution using one-stage growth. Uemura *et al.*[14] report that sheaf-like crystals are observed at a one-stage isothermal T_c of 167°C, and at more concentrated polymer solutions of 0.1 wt%.

The self-seeding technique to grow PE single crystals[18,21] has been well studied, and results showed that the number and nature of seed crystals were determined primarily by the seeding condition. For Ryton V-1, increasing T_e from 199 to 201°C (the solution clearing point is ~197°C), resulted in the growth of PPS single crystals. At T_e = 199°C, only sheaf-like crystals were observed; no single crystals were observed at this low T_e (as shown in *Figure 2a*). When T_e was increased to 200°C, single crystals can be seen along with the coexisting sheaf-like crystals. Although single crystals were able to

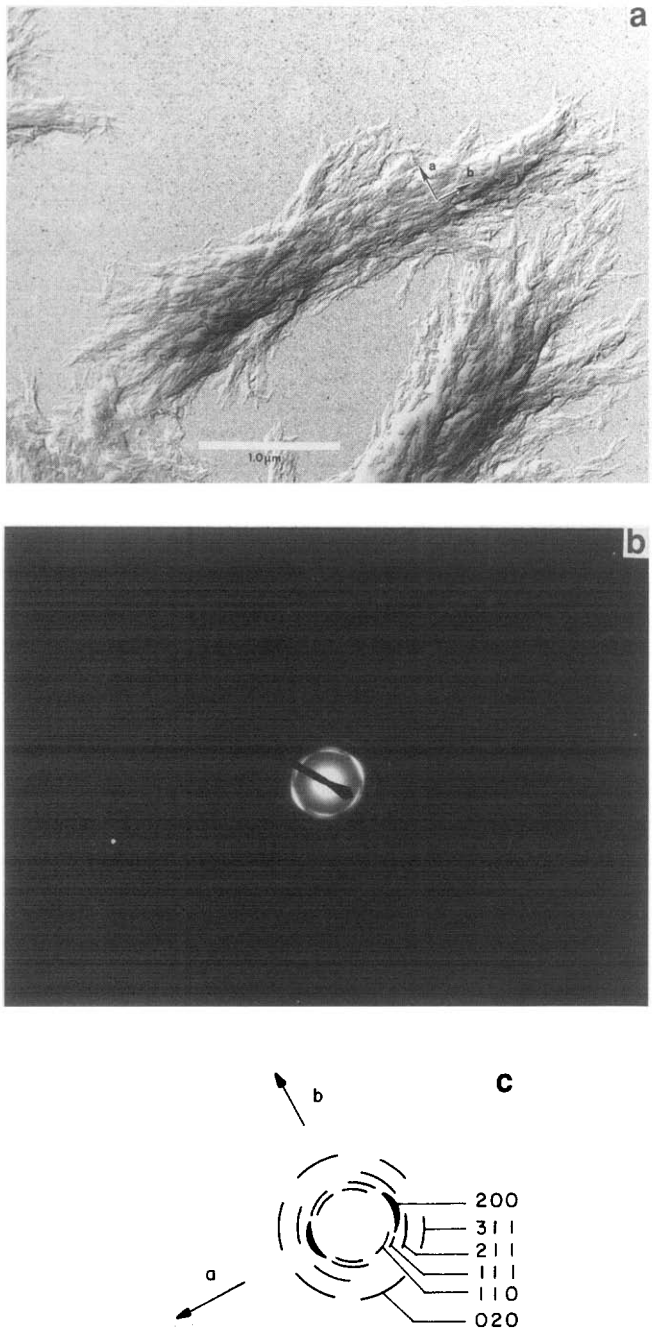

Figure 2 (a) Typical TEM micrograph of sheaf-like aggregate crystals of Ryton V-1 PPS which have been grown at $T_e = 199°C$ and $T_c = 180.0°C$. (b) Arc-like diffraction pattern from the area in (a) beneath the arrows. (c) Sketch of the pattern in (b) with arcs indexed

be formed at this T_e, the morphology of the single crystals revealed star-like aggregates in which three or four single crystals grew from the same seed. Apparently the size of seed crystals is determined by T_e and will be a dominant effect in the formation of single crystals. The formation of star-like single crystal aggregates is not due simply to the overlap of several single crystals together, because these star-like single crystal aggregates have never been observed at a T_e other than 200°C. When T_e was further increased to 201°C for Ryton V-1, followed by isothermal crystallization in the range of 166.5–185°C, only single crystals were observed; the sheaf-like crystals were absent. *Figure 4* shows the TEM micrograph of Ryton V-1 PPS single crystal grown by using the self-seeding technique with $T_e = 201°C$ and $T_c = 166.5°C$. The electron diffraction pattern of the solution grown crystal, shown in *Figure 5*, revealed the nearly spot-like diffraction pattern of a typical single crystal. Further increase in T_e resulted in very slow crystal growth. An attempt to raise T_e to 202°C resulted in only a very small amount of crystals forming after 7 days at $T_c = 180°C$.

We could not observe the actual seed crystals present in the solution at elevated temperature. We attempted to reduce the solution concentration sufficiently to prevent crystallization during cooling, so that we could capture the seed crystals. However, even after diluting the solution by more than a factor of forty, crystallization was initiated on the seeds. The nature of the seed crystals surviving at 201–205°C is still unknown.

Although T_e is the dominant factor affecting the morphology of solution grown crystals, depending upon the material used T_c may also affect the morphology of solution grown PPS crystals. The morphology of the crystal grown from film grade PPS, which is a medium molecular weight branched polymer, was only affected by T_e and was not affected by T_c in the range studied. However the morphology of the solution grown Ryton

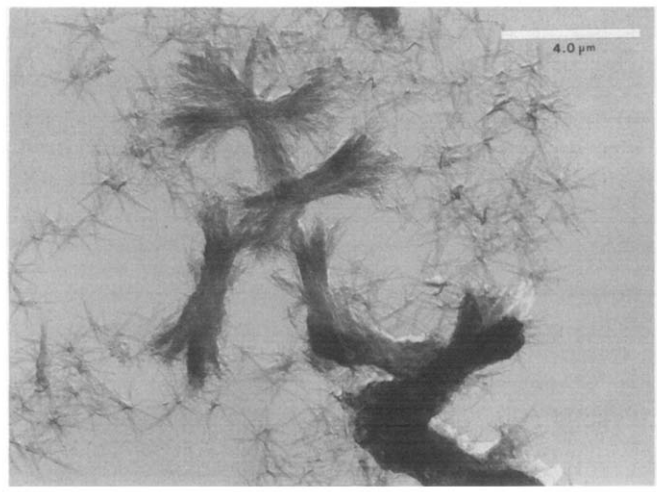

Figure 3 Typical TEM micrograph of the coexistence of the sheaf-like aggregates and star-like single crystal aggregates of Ryton V-1 PPS which have been grown at $T_e = 200°C$ and $T_c = 180.0°C$

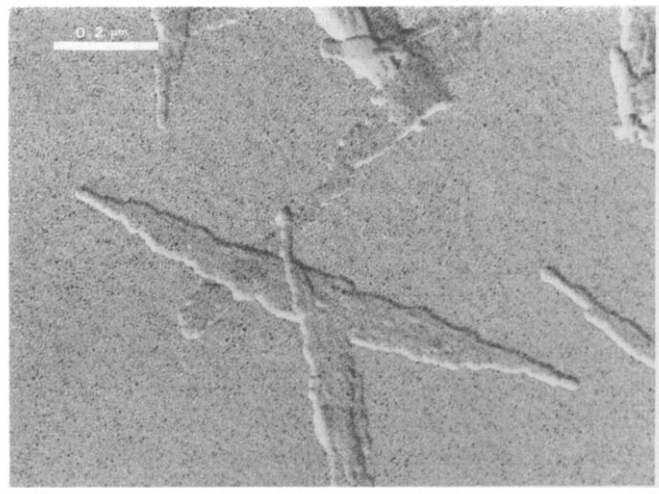

Figure 4 TEM micrograph of a Ryton V-1 PPS single crystal grown at $T_e = 201°C$ and $T_c = 166.5°C$

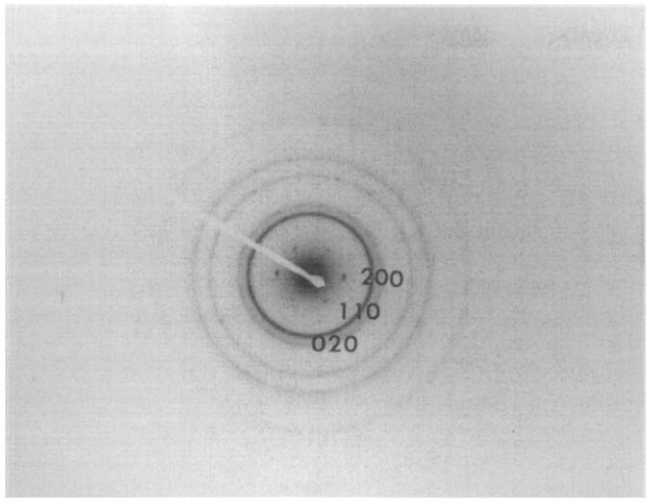

Figure 5 Spot-like electron diffraction pattern from Ryton V-1 PPS single crystal grown at $T_c = 201°C$ and $T_c = 166.5°C$, showing (200), (110) and (020) diffraction spots

Figure 6 TEM micrograph of a Ryton V-1 PPS big crystal grown at $T_c = 201°C$ and $T_c = 175°C$

V-1 PPS crystals was more complicated and was affected not only by T_c but also by T_c. Although sheaf-like aggregates were no longer observed for Ryton V-1 and only needle-like single crystals were formed when T_c was set at 201°C, a third type of crystal can be seen. This third type of crystal morphology is different from the sheaf-like aggregates and needle-like single crystals. The dimensions of these crystals, which we have called 'big' crystals, are in the range of 1–3 μm long, 0.4–0.5 μm wide and ~20–70 nm thick. A typical TEM micrograph of a big crystal can be seen in *Figure 6*. For comparison, the dimensions of single crystals are 1–3 μm long, 0.1–0.3 μm wide and 7–10 nm thick, and in the case of sheaf-like crystals 2–6 μm in length, 1–2 μm wide and 30–100 nm thick. *Figure 7* shows a sketch of the relative size and shape of these three types of Ryton V-1 solution grown crystals. In general the needle-like crystals have a fold surface texture showing some striations along the long axis, but the diffraction pattern is still spot-like. However, the big crystals are generally not as well oriented as the single crystals, and microfibrillar texture on the crystal surface can be observed.

The population of big crystals is a function of T_c. The higher the T_c used, the greater the population of this third type of crystal. Most often the electron diffraction pattern of a big crystal showed several sharp arcs but occasionally the single crystal like spot diffraction pattern was seen. The arc-like diffraction pattern showed that these microfibrillar textures inside the big crystals aligned parallel to the long direction of the crystals, and the occasionally observed spot diffraction patterns of some big crystals suggested that these particular aggregates have the characteristics of single crystals.

Effect of crystallization temperature

In *Figures 8a–d*, single crystals of film grade PPS are shown for $T_c = 205°C$ and $T_c = 170.0$, 175.0, 180.0 and 182.5°C, respectively. Different shadowing materials were used (Au/Pd for *Figure 8a–c*, and Au for *Figure 8d*), and this accounts for the different grain sizes in *Figure 8*. Film grade single crystals are similar to those grown from Ryton, showing needle-like lamellar habit and irregular lateral edges. However, at the highest T_c the film grade material produces crystals which were so long and narrow that their lamellar character was obscured. Spot-like diffraction patterns, rather than arcs, were seen from these film grade single crystals (and, indeed, from all true PPS single crystals grown by the two-stage self-seeding method), similar to the spot-like diffraction shown in *Figure 5*. Only ($hk0$) reflections are seen, indicating that the c-axis is parallel to the direction of the electron beam. The b-axis is aligned along the long dimension of the crystal, which we define to be the growth direction for PPS single crystals. From an examination of many single crystals grown at different T_cs, we find that PPS crystals show no tendency for sectorization. When crystals split, they do so along the b-axis growth direction. We observed no faceting of the crystals, a result supported by the observations of Lovinger[12,13] for PPS crystals grown by one-stage crystallization at 150°C. The anisotropy of the crystal habit is strongly affected by T_c.

The film grade material is an experimental product, and may not be as clean as the commercial grade Ryton V-1 product. Evidence for existence of impurities can be seen at the edges of several needle-like crystals shown in

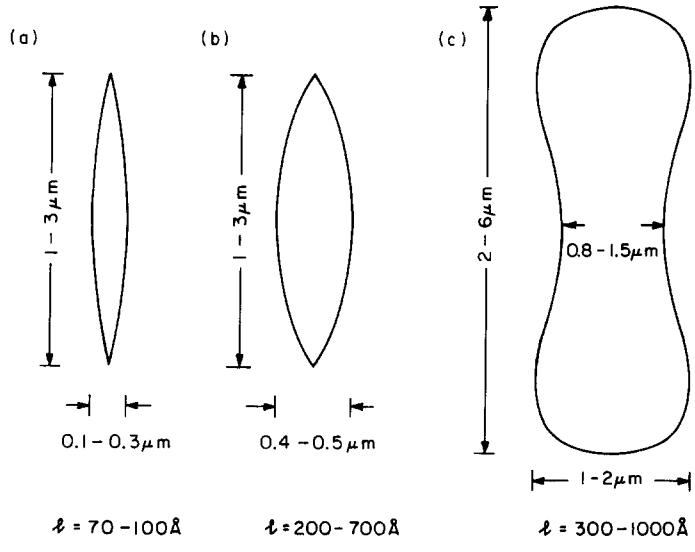

Figure 7 Sketch of the relative size and shape of PPS solution grown crystals: (a) single crystals; (b) big crystal; (c) sheaf-like aggregate

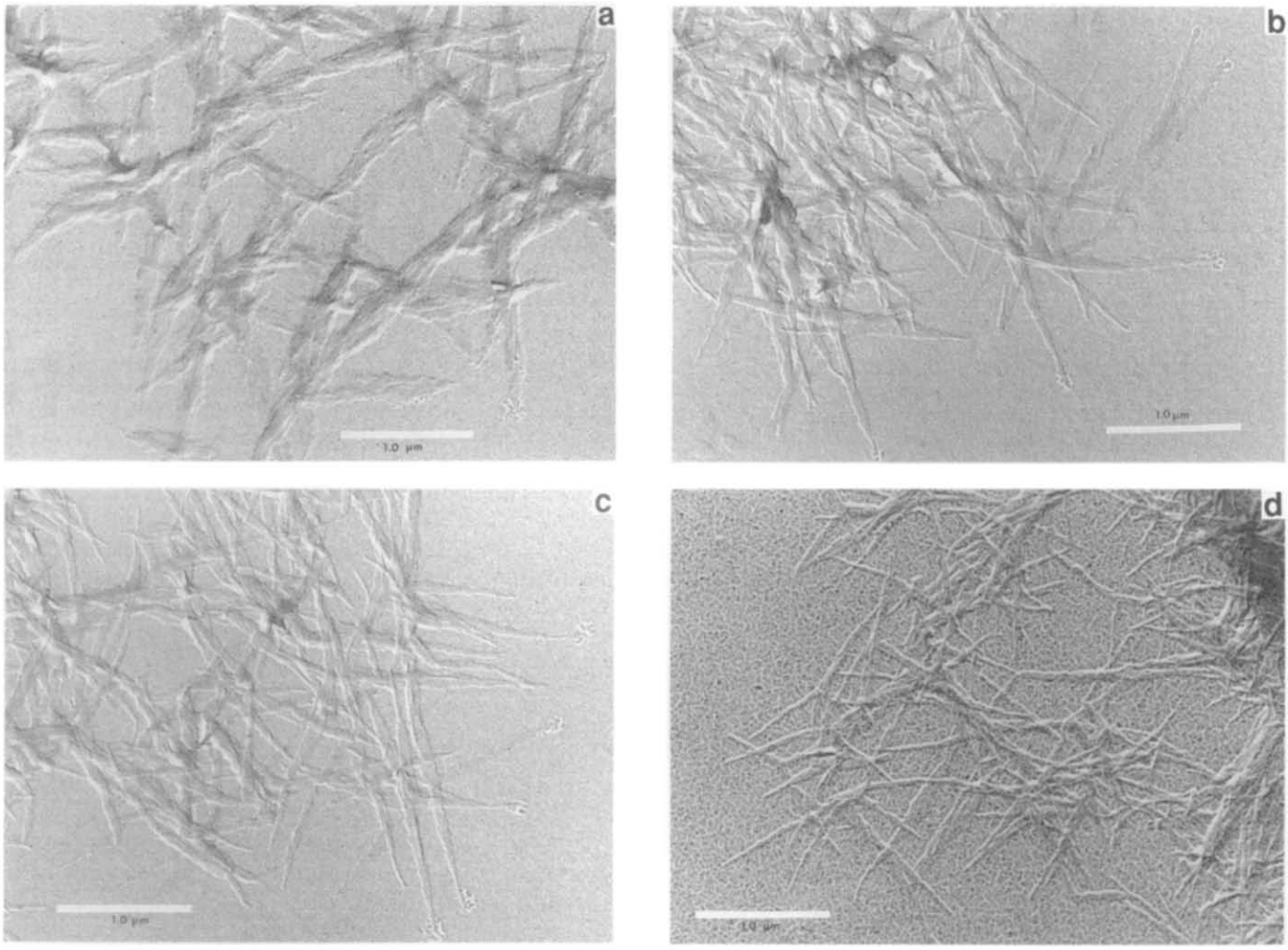

Figure 8 TEM micrographs of film grade PPS single crystals grown at $T_e = 205°C$ and T_c: (a) 170.0°C; (b) 175.0°C; (c) 180.0°C; (d) 182.5°C

Figure 8. Here, impurities in the solution tended to wet the polymer crystal, collecting at the crystal tips when the solvent was evaporating. This impurity component caused the gold shadowing material to deposit in larger grains at the crystal tips.

To characterize the dimensions of needle-like crystals of Ryton V-1 and film grade PPS we use the aspect ratio, which is defined as the ratio of the crystal length in the *b*-direction to that in the *a*-direction. To account for differences in T_c, the two materials have been compared on the basis of undercooling, which is defined here as the difference between T_e and the second-stage T_c ($\Delta T = T_e - T_c$). A plot of aspect ratio *versus* undercooling is shown in *Figure 9*. The determination of aspect ratios has been done by averaging >60 individual crystal measurements. To avoid local aggregation effects, several TEM specimens were prepared for each sample in order to cover all possible crystals. The error range from averaging the results from different TEM specimens is ± 3–5%, and is smaller than the variation of the aspect ratio of the PPS single crystal itself.

Analysis of single crystal mats

The d.s.c. peak maximum temperatures and heats of fusion for Ryton V-1 and film grade PPS single crystal mats are shown in *Table 1*. Heats of fusion differ between the two materials, with Ryton V-1 mats having an average lower heat of fusion than film grade mats. D.s.c. endotherms are shown in *Figures 10a* (Ryton V-1) and *b* (film grade) and the plots of the melting peak temperatures of both grades of PPS *versus* T_c are shown in *Figures 11a* and *b*. The d.s.c. scans in *Figure 10* have been normalized to units of cal g^{-1}, to allow a direct comparison of samples of different mass. Ryton V-1 mats show a double endothermic response at the three lowest T_cs. A shoulder appears on the high temperature side of the d.s.c. endotherm for $T_c = 180°C$, and by $T_c = 182.5°C$, only a very broad single endotherm is seen. For film grade mats, no clear dual endothermic response is seen, though a shoulder appears on the low temperature side of the endotherm for $T_c = 182.5°C$. Film grade mats have a broader distribution of crystal melting points, judging from the point of first departure from the baseline, which occurs near ~240°C in film grade mats compared to ~260°C in Ryton V-1 mats. The peak T_ms are about the same for Ryton V-1 mats and film grade mats and for the latter do not vary in a consistent manner with T_c. Thus, while crystal habit differs markedly for different degrees of undercooling, this is not reflected in the endothermic behaviour of mats prepared from single crystals.

Variability in the dependence of endothermic response (peak temperatures and heats of fusion) on T_c may come from two sources. First, if the uncrystallized fraction is not totally removed, the precipitate will contain less

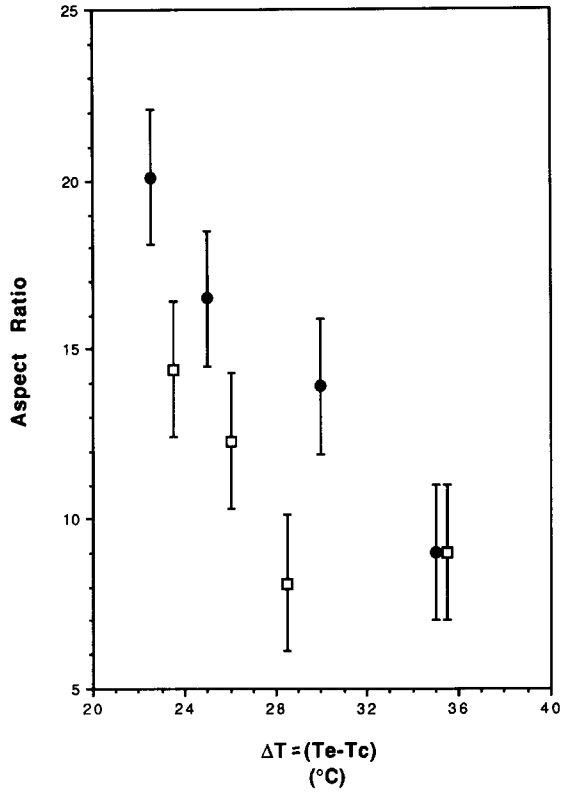

Figure 9 Aspect ratio of both grades of PPS single crystals *versus* the undercooling, defined as the seeding temperature (T_c) minus the crystallization temperature (T_c): (□) Ryton V-1; (●) film grade

Table 1 Endotherm peak maximum temperatures and the heat of fusion for PPS single crystal mats crystallized at T_c

Sample type	T_c (°C)	T_m (°C)		ΔH (J g^{-1})
R[a]	172.5	287.4	290.9	64.7
R	175.0	286.8	290.3	65.0
R	177.5	287.4	293.0	65.2
R	180.0	289.5		69.9
R	182.5	292.3		66.4
F[b]	170.0	288.8		67.1
F	175.0	286.7		73.6
F	177.5	288.3		69.6
F	180.0	288.2		68.2
F	182.5	290.8		67.3

[a]Ryton V-1 powder, 0.02% concentration, 140°C first-stage crystallization, 201°C T_c

[b]Film grade powder, 0.02% concentration, 140°C first-stage crystallization, 205°C T_c

perfect crystals that broaden the endotherm and decrease the T_m. Second, impurities in the starting materials affect the T_m and degree of crystallinity in the mats of single crystals. We developed an extensive ion-extraction and washing procedure* to remove organic and inorganic impurities. When this procedure was used, and when the uncrystallized fraction was carefully removed from the solution prior to precipitating the mats, the crystal melting points increased with T_c in a regular manner. The d.s.c. endotherms of these purified Ryton V-1 single crystal mats are shown in *Figure 12a* and plots of T_m *versus* T_c are shown in *Figure 12b*. With a reduction in the impurities which will alter the crystallization kinetics, both the higher and the lower melting peak temperatures increase steadily as the second-stage T_c increases. We note, however, that these cleaning procedures did not alter the morphology of the resulting single crystals.

By using a least squares method of fitting, the crystallographic *a*-, *b*- and *c*-axis lattice parameters were calculated from the 2θ angles. We assumed the orthorhombic structure proposed by Tabor *et al.*[3] and used the angular positions of the (1 1 0), (1 1 2), (2 1 1), (0 2 0) and (3 1 1) reflections. The lattice parameters of the PPS single crystals are related to the isothermal T_c. For the

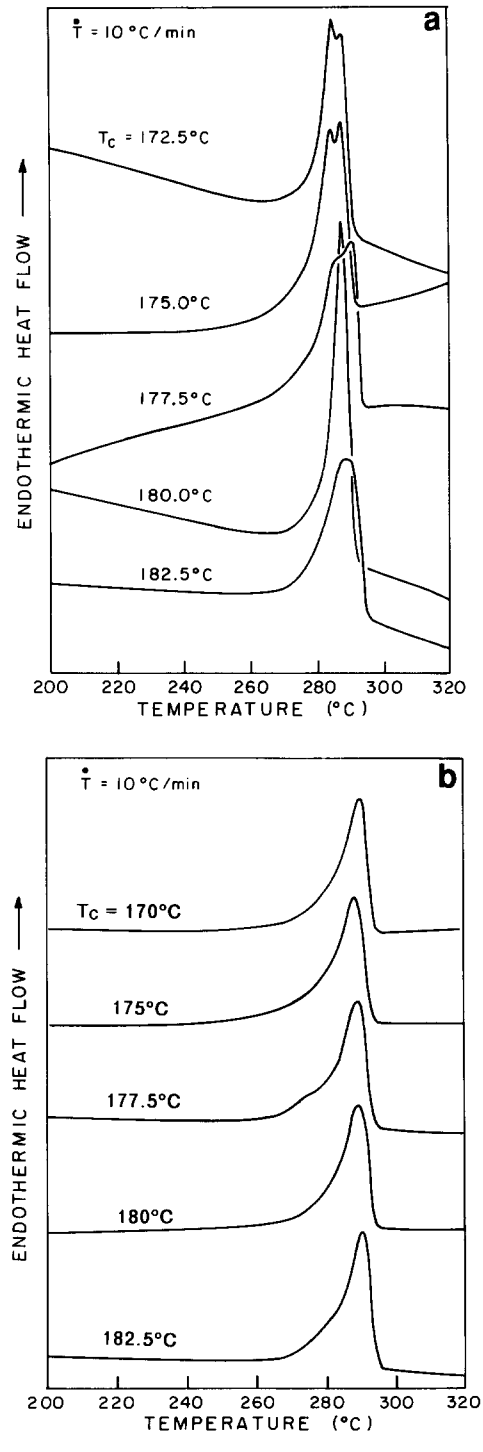

Figure 10 Collective melting endotherms of the single crystal mats from (a) Ryton V-1 PPS grown at T_c = 201°C and T_c as indicated and (b) film grade PPS grown at T_c = 205°C and T_c as indicated. The vertical axis is in arbitrary units, but each scan has been normalized to heat flow per unit mass

* Washing procedures include stirring PPS powder in 1M HCl aqueous solution at 90°C, refluxing in ethylene glycol, and then extensively washing in organic solvents

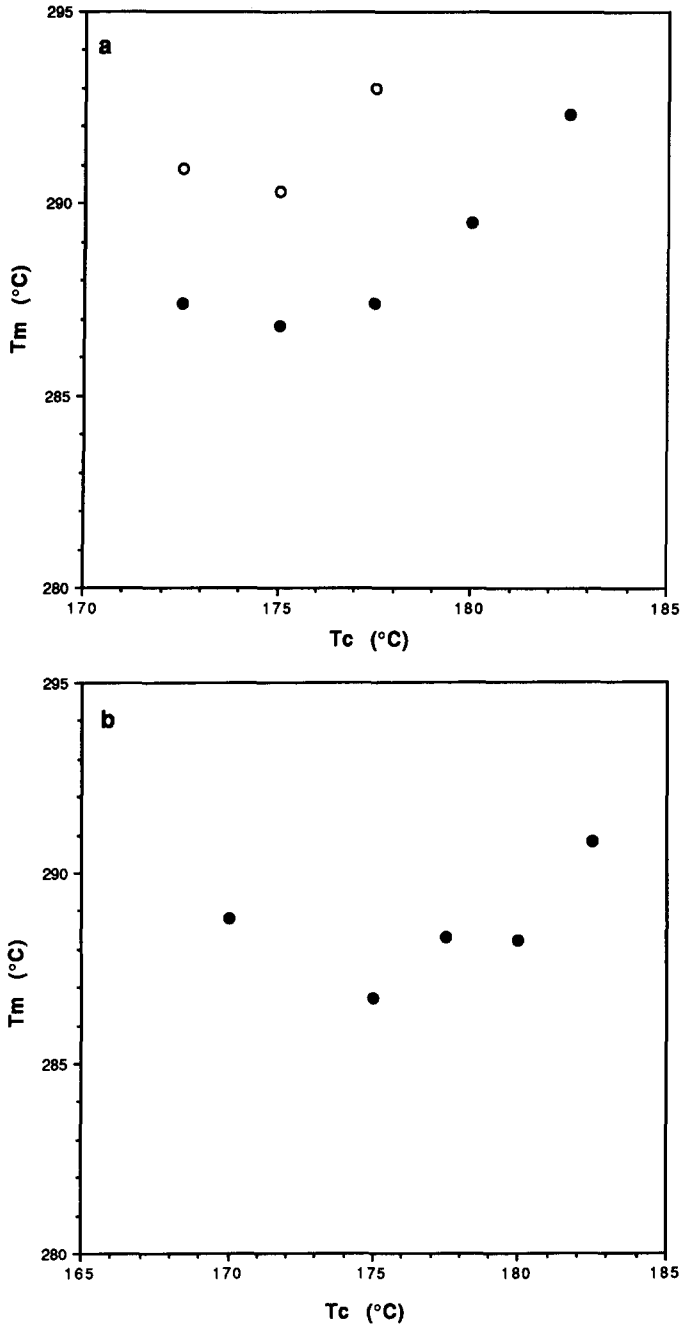

Figure 11 Melting peak temperatures of the single crystal mats *versus* the crystallization temperature of (a) Ryton V-1 PPS seeded at $T_c = 201°C$ and (b) film grade PPS seeded at $T_c = 205°C$: (●) T_m1; (○) T_m2

Ryton V-1 single crystal mats, the *b*-axis does not vary with T_c, but both *a* and *c* decrease as T_c increases. The value of the lattice parameters are:

$T_c = 172.5°C$ $a = 0.864$ nm $b = 0.562$ nm $c = 1.024$ nm

$T_c = 182.5°C$ $a = 0.856$ nm $b = 0.561$ nm $c = 1.017$ nm

This results in an increase in crystal density from 1.442 g cm^{-3} at $T_c = 172.5°C$ to 1.476 g cm^{-3} at $T_c = 182.5°C$. The values of the lattice parameters and crystal density for the Ryton V-1 single crystals fall within the range of values[3–5] cited by others for melt crystallized Ryton V-1.

PPS crystals decorated with PE

The direction of the fold plane in PPS single crystals was the subject of an experiment utilizing the PE decoration method of Wittmann and Lotz[22]. Semi-crystalline polymers can be pyrolysed into short chain oligomers and are able to crystallize when deposited onto the substrate surface. If the substrate surface has a unique topological feature, the pyrolysed short chain oligomers may be able to pack into the channels and initiate crystallization to form decoration rods. By utilizing the orientation of decoration rods, the surface topology may be revealed. Wittmann and Lotz deposited vapours of pyrolysed PE which actually is low molecular weight paraffin (4000 g mol^{-1}) onto the fold surface of a variety of polymer crystal substrates. The PE chains in the vapour deposited on substrates and crystallized to form tiny rods, which were observed using TEM. By assuming

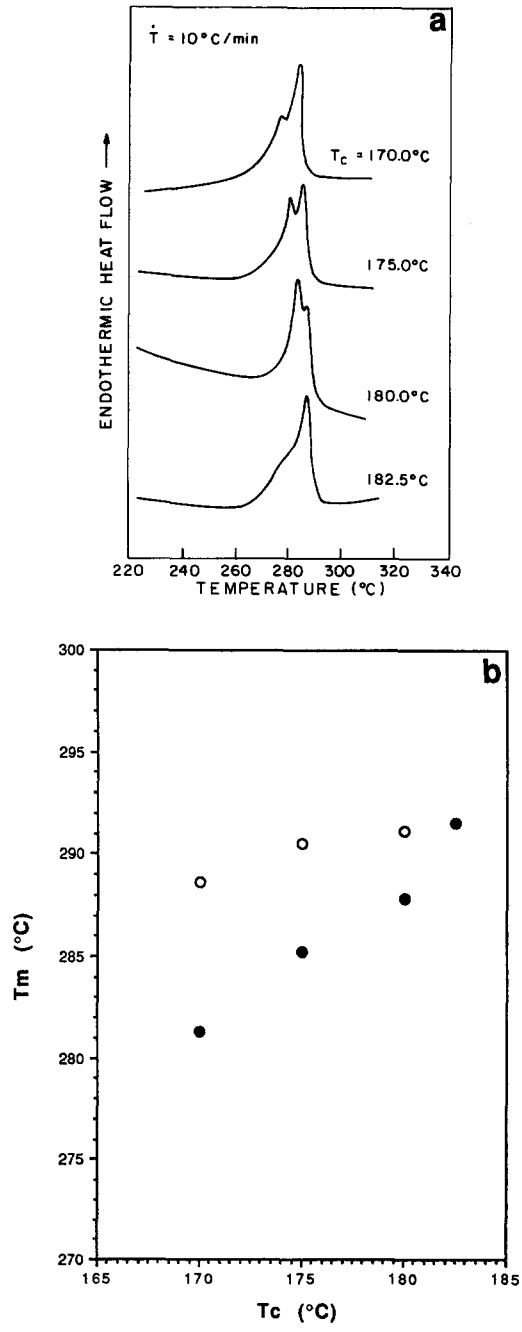

Figure 12 (a) Collective melting endotherms of the purified Ryton V-1 PPS single crystal mats grown at $T_c = 201°C$ and T_c as indicated. (b) Melting peak temperatures of purified Ryton V-1 single crystal mats *versus* the crystallization temperature: (●) T_m1; (○) T_m2. The vertical axis is in arbitrary units, but each scan has been normalized to heat flow per unit mass in (a)

the polymer chains fold along the PE single crystal in a tight fold, the decoration polymer chain will initially pack into the channel between the fold plane and further initiate crystallization to form the tiny decoration rods. The dimension of these decoration rods is ~20 nm in diameter and 200 nm in length. While the individual decorating chains themselves oriented in the fold plane of the substrate crystal, the observed rods aligned perpendicular to the fold plane. Wittmann and Lotz interpreted the orientation of the decorating rods on a sectored PE single crystal as evidence that the fold plane was parallel to the growth front of the single crystal.

We vapour deposited several semicrystalline polymers, such as PE, isotactic polypropylene and poly(vinylidene fluoride), onto PPS single crystals, then shadowed with Au or Au/Pd. Decoration results from poly(vinylidene fluoride) and isotactic polypropylene did not reveal any specific features. These decoration rods on PPS single crystal surface did not orient in any particular direction. However, the decoration rods from pyrolysed PE did align in a particular direction. *Figures 13a* and *b* show the TEM micrographs of PE decorated Ryton V-1 PPS single crystals that were grown at T_c = 166.5 and 175°C, respectively. In the lower left region of *Figure 13a*, the PE decoration rods randomly deposit on the support carbon film and there is no preferred orientation of the

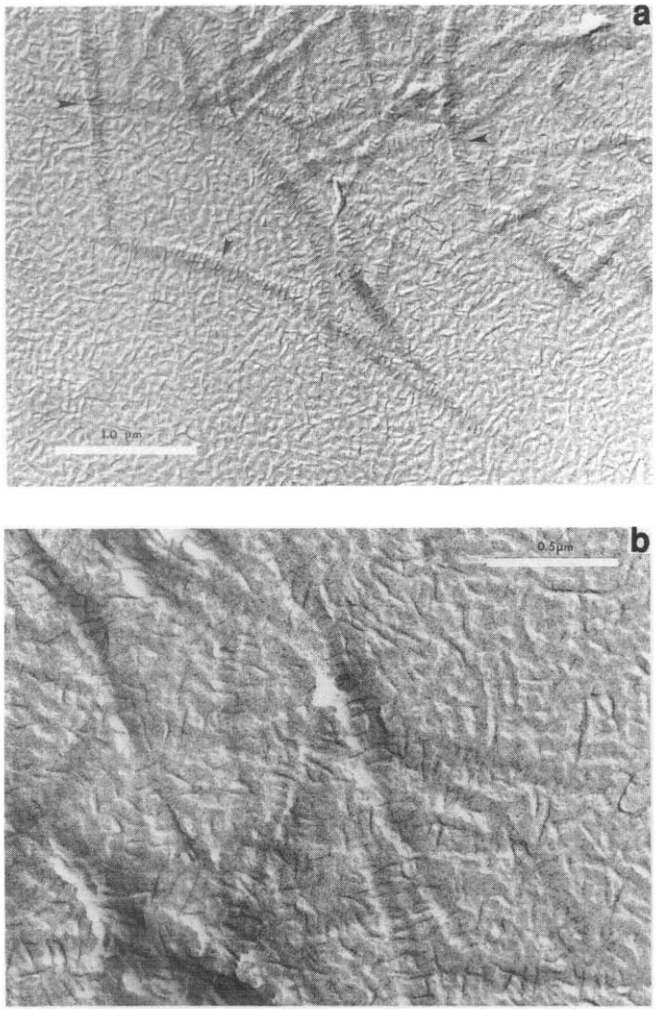

Figure 13 TEM micrograph of PE decorated Ryton V-1 PPS single crystals seeded at T_e = 201°C and crystallized at (a) T_c = 166.5°C and (b) T_c = 175.0°C. Areas showing preferred orientation of the decoration PE rod on the single crystal surface are marked by arrows in (a)

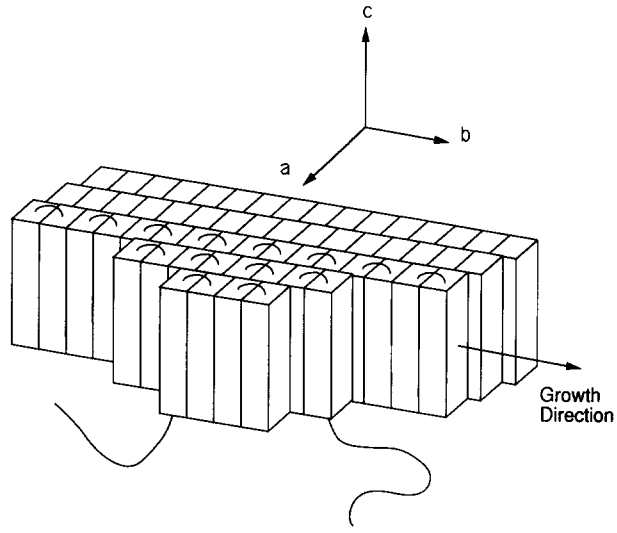

Figure 14 Sketch of the suggested polymer chain folding direction in PPS single crystals in which the PPS molecules fold parallel to the crystal growth direction which is also the long dimension of the needle-like single crystal

PE decoration rod. The preferred orientation of the decoration rods on the crystal surface is marked by arrows in *Figure 13a*. The long needle-like crystal running at ~45° just left of the centre in *Figure 13a* is most likely several crystals overlapped end-to-end. When the pyrolysed PE molecules deposited and crystallized on the needle-like PPS single crystals, however, the decorating rods on the crystal surface have a predominant orientation: these rods align perpendicular to the long dimension of the crystal. The outlines of the PPS crystals are obscured because the decorating rods are quite large compared to the PPS crystals, and very often the rods span the entire crystal width. The size of the PE decorating rod is ~0.2 μm long, very comparable to the rod size in Wittmann and Lotz's decoration of PE single crystals[22]. Because PPS crystals are very much smaller than the crystals of PE, polyoxymethylene and isotactic polypropylene studied by Wittmann and Lotz[22], and the PPS single crystals have a tendency to aggregate together, we were unable to obtain the spot-like PPS diffraction along with the (002) diffraction from PE decoration rods. However assuming Wittmann and Lotz's theory of the effect of substrate folds on rod orientation is generally correct, we would conclude that in PPS crystals, the fold plane is perpendicular to the *a*-axis and parallel to the *b*-axis growth direction. This is shown schematically in *Figure 14*.

DISCUSSION

PPS solution grown crystals

The growth of PPS single crystals from dilute solution was first reported by Lovinger *et al.*[12,13] using the one-stage isothermal crystallization method. These solution grown crystals have a needle-like habit and have very rough fold and growth surfaces. Instead of revealing the characteristic spot pattern of single crystals, only a broad arc electron diffraction pattern has been reported which indicates these needle-like solution grown crystals were actually multiple crystalline aggregates. The length of these crystals is generally 1–3 μm and their overall width is ~0.1–0.3 μm. However, careful inspection of

the surface textures on these needle-shaped PPS crystals reveals that these crystals are actually composed of much narrower microfibrillar crystals[12–15,23], whose width (~15–20 nm) is only slightly larger than their thickness (~10–15 nm). Here, we have used a two-stage self-seeding method to grow PPS single crystals. The results of spot-like electron diffraction and improved smoothness of the crystal fold surface are evidence that combining the two-stage self-seeding technique with careful removal of the uncrystallized fraction is a better method to grow PPS single crystals.

The morphology and melting behaviour of the PPS solution grown crystals have also been reported by D'Ilario *et al.*[16,17,24,25]. The Ryton V-1 aggregated crystals were grown[16,17] from diphenyl ether dilute solution by using the one-stage technique at temperatures ranging from 151.0 to 211.8°C. They reported[16] that the long spacing of the solution grown crystal lamellae is ~28 nm and is independent of T_c. The 28 nm thickness of the PPS crystals indicates that the PPS chain only folds once to form the lamellar crystal. This is about three times thicker than the lamellar thickness estimated (~7–10 nm) from TEM micrographs of our more perfect PPS single crystals. However D'Ilario and Piozzi suspected that the spacing measured from small angle X-ray scattering may be attributed to other morphological features of their grown crystals. They also reported[24] that double melting peaks have been observed when T_c is lower than 210°C, but only one broad melting endotherm can be seen when T_c is 211°C.

There are some differences in the two-stage self-seeding technique between Ryton V-1 and film grade PPS. The T_e is 205°C for film grade PPS, 4°C higher than the T_e required for Ryton PPS. We also found that the time required for the film grade solution to become opaque during first-stage crystallization is shorter than the time required for the Ryton V-1 indicating faster solution crystallization kinetics for the branched, medium molecular weight material. The higher T_e of film grade PPS suggests that the film grade PPS is able to form more perfect crystals than Ryton V-1 after first-stage crystallization. The time required to observe the opacity of the solution at the first-stage crystallization for film grade is ~2.5 h, where it is ~4 h for Ryton V-1. However, when we investigated the melt crystallization, and melting behaviour, of both Ryton V-1 and film grade PPS, we found[26] the film grade has a much slower melt crystallization kinetics and a lower T_m (~4°C lower) than Ryton V-1 after crystallization from the melt. Comparing the crystallization behaviour from both melt and dilute solution, it shows that the crystallization kinetics and the perfection of grown crystals may have different material dependency. For example, the crystal perfection of crystals grown from film grade PPS is higher than that of Ryton V-1 when the crystal is grown at dilute solution because of the molecular weight effect. But the perfection of melt grown crystals of film grade PPS is lower than that of Ryton V-1 due to chain branching effects.

The crystal habit in PPS is strongly affected by T_e. Unless a high enough T_e is used to produce small enough seeds, sheaf-like multiple crystalline aggregates or star-shaped single crystal aggregates will be formed. Microfibrillar ribbons can be seen on the fold surface and growth edges of the sheaf-like multiple crystalline aggregates. Each microfibrillar ribbon is representative of a local crystal growth. In general, the sheaf-like crystal is observed under high growth rate and high nucleation rate conditions, such as large undercooling and low T_e. Four- to six-arm sheaf-like multiple crystalline aggregates have been observed after one-stage crystallization of both Ryton V-1 and film grade at 140°C. The formation of sheaf-like multiple crystalline crystals may be due either to a too fast crystal nucleation rate at a large undercooling or to too many nucleation sites on the crystal seeds at low T_e.

The crystal habit and morphology may also be affected by the type of materials and the T_c. When the T_e was high enough, the 'big' crystals, along with single crystals, were observed regardless of the T_c for the Ryton V-1. But what we have called the 'big' crystals have never been observed in film grade samples. Ryton V-1 PPS has been reported[20] to contain a lot of low molecular weight oligomers which cannot be removed completely by Soxhlet extraction. In our experience, after 2 days of Soxhlet extraction of Ryton V-1 by THF solvent, a certain amount of the PPS, presumably oligomers, was extracted and then precipitated in the bottom of the flask. However, there are no precipitates extracted from film grade even after 7 days of extraction. This observation, combined with the faster crystallization of higher molecular weight materials, leads to an explanation for the occurrence of 'big' crystals in Ryton V-1. We suggest that the formation of the 'big' crystals is due to the low molecular weight fraction in Ryton V-1 which crystallizes onto already formed premature single crystals (made from the higher molecular weight fraction) and then acts as 'glue' to combine the premature single crystals to form aggregate flat crystals. Our electron diffraction experimental results showed the sharp arc pattern was observed for most of the 'big' crystals, but the spot pattern can also be seen occasionally. Due to the anisotropy of PPS crystal habit the prematurely grown crystals have a tendency to align in roughly the same direction to form aggregates, resulting in the arc-like diffraction. However the spot-like electron diffraction pattern was sometimes observed perhaps indicating that these 'big' crystals have been well grown and aligned in the same direction.

With regard to the endothermic response of mats of single crystals, it is tempting to try to interpret the existence of dual endotherms in Ryton V-1 by the existence of dual crystal morphologies (single crystals coexisting with big crystals or with sheaf-like crystals). However, in another case, crystals prepared from a single-stage isothermal crystallization at 140°C (first-stage crystallization only) showed four- to six-armed sheaf-like aggregates but have a triple melting endotherm. Dual endotherms were also observed from the crystal mats grown at low T_e where only a single morphology of sheaf-like aggregates was observed. By carefully comparing the dual melting peak temperatures and peak height of the cleaned-up Ryton V-1 PPS samples (*Figure 11*) as a function of T_c, we observe that the lower melting peak shifts to a higher temperature and increases its peak height as T_c increases. The higher melting peak temperature only slightly increases as T_c increases, and its peak height is reduced as T_c increases. When T_c is raised to 182.5°C, the lower melting endotherm shifts to a higher temperature and becomes a dominant peak, and the upper melting peak diminishes to form a shoulder. One of the very important features of the melting behaviour of Ryton V-1 solution grown crystals is that the dual endotherms have always been found at low T_c but only

a single broad melting endotherm has been found at high T_c, regardless of the material clean-up process, the T_c or the solvent used. This, and dual endothermic behaviour converting to a single endotherm, takes place when T_c is ~180°C for 1-chloronaphthalene solvent and ~210°C for diphenyl ether solvent[24]. The formation of sheaf-like crystal aggregates does not affect the single–dual melting transition; however it will lower the melting point compared to that of the single crystals.

These results from the melting study of the PPS solution grown crystals suggest that reorganization may play a role in the dual endothermic response. We would expect that single crystals may reorganize more easily than melt crystallized polymer due to the absence of geometrical constraints. It has been well documented that single crystals of PE[27,28], polyoxymethylene[29], and isotactic polystyrene[30], are very easily subjected to reorganization during normal d.s.c. scans because of their chain-folded lamellar characteristics. When the single crystal is grown at a higher temperature, a larger lamellar thickness is expected and a higher melting peak temperature is also expected. As the perfection of the single crystals improves with increasing T_c, the real melting endotherm will shift to a higher temperature and the chance for reorganization or annealing should be suppressed. We have observed that the lower melting peak of the PPS single crystal mats shifts to a higher temperature and the area underneath this peak increases as T_c increases. We also observed the higher melting peak temperature slightly increases as T_c increases, however the area underneath this peak decreases as T_c increases. This T_c dependency of the dual melting behaviour of the cleaned-up Ryton V-1 single crystal mats and the multiple melting behaviour of the sheaf-like solution grown crystals may suggest that the solution grown PPS single crystals can undergo reorganization or annealing during d.s.c. scans. A similar result has also been found in Soxhlet-extracted Ryton V-1 single crystal mats (*Figure 10a*), although the T_c dependency of the dual melting behaviour does not show a regular trend. For the film grade PPS (*Figure 10b*), the ability of reorganization may be restricted due to the chain branching effect, therefore the dual melting endotherm may not be observed. The reorganization peak may be too small and may overlap with the real melting endotherm in film grade PPS.

PPS single crystal aspect ratio

Unlike PE single crystals that reveal discrete fold sectors and distinct crystal habits, PPS single crystals show axially anisotropic needle-like crystals with rough edges. The axial anisotropy of the PPS single crystals is strongly related to the T_c and molecular weight. As the T_c or molecular weight increases, the axial anisotropy increases and the aspect ratio of the needle-like single crystal increases.

The morphology of lath- and needle-shaped single crystals has been reported for a wide variety of polymers[31–43] in addition to the engineering thermoplastics poly(ether ether ketone) (PEEK)[44–47] and PPS[5,12–17]. The variation of aspect ratio with T_c in PPS may be compared to that seen in other polymers. The crystal habit and aspect ratio of solution grown single crystals of PE is a function of the T_c[18,19,21,48–54]. The single crystal habit changes from lozenge to truncated lozenge and to elongated curved crystal as T_c increases. In early work at lower T_cs the aspect ratio of the PE single crystal increased with T_c, and ranged from 1 to ~4.3. Later work showed that an aspect ratio of up to 6 could be achieved at even higher T_cs[49]. A similar relationship is also observed in both Ryton V-1 and film grade PPS single crystals. However, the aspect ratio for PPS is extremely high, reaching 20 for film grade and 14 for Ryton V-1 at the smallest undercoolings. This is comparable to the aspect ratio of single crystals of poly[bis-(2,4-dichlorophenoxy)-phosphazene][43]. The aspect ratios of the Ryton V-1 and film grade PPS single crystals decreased as the degree of undercooling increased. We attempted highly to undercool Ryton V-1 in an effort to obtain crystals with faceted growth and a much smaller aspect ratio, but found that the aspect ratio levelled off at the highest undercooling ($\Delta T \sim 35$°C). It was not possible to obtain a crystal from Ryton V-1 with an aspect ratio below 8. Degrees of undercooling greater than $\Delta T \sim 35$°C could not be explored because we were unable to cool the solutions fast enough.

Fold plane direction in PPS single crystals

Our suggestion that PPS single crystals have their fold planes parallel to the long dimension finds a precedent in much of the early work. Geil's observation[31] that the hydrogen-bonded sheets are parallel to the long dimension in nylon 66 led Dreyfuss and Keller to conclude that the fold plane is along the lath direction[41]. Keith *et al.*[39] arrived at the same conclusion for single laths of poly(1-glutamic acid) (PG) when these were grown from the barium salt of PG. Mechanical deformation of lath-like crystals has resulted in fibrils spanning the cracks when the crack runs parallel to the lath short dimension in polypropylene[33], poly(1-butene)[37], and in isotactic poly(3-methyl-1-butene)[36]. The existence of these fibrils was in each case taken as evidence of chain unfolding during deformation, thus leading to the conclusion that the fold plane is along the longer dimension of the crystal.

Lovinger and Davis[45], in earlier work on PEEK, predicted the likelihood of cleavage of (2 0 0) planes based on the backbone orientation with zigzag planes parallel to the growth direction (*b*-axis). Recently, Waddon *et al.* observed that PEEK crystals do tend to cleave along the direction of growth[46]. Easy cleavage along the lath suggests that this is the direction along which no primary bonds are broken, and hence is the direction of the fold plane. In PPS single crystals, we have also observed splitting predominantly along the *b*-axis growth direction. This evidence, coupled with lack of sectorization, lack of macroscopic faceting, and observation of PE decorating rods lying transverse to the growth direction, all point toward a fold plane which lies along the growth direction.

Anisotropic PE crystals without any sectors can be grown at temperatures higher than 120°C from dilute solution or from molten paraffin used as a solvent[51]. Comparing the morphology between PPS and PE elongated crystals, there exists some similarity and dissimilarity. First both PPS and PE crystals show the needle shape, (floreate shape was suggested for PE by Keith[51,52]) although the aspect ratio of PPS is much higher than that of PE. Another very interesting similarity is the polymer fold direction. The PE single crystal grown at high temperature resulted in non-faceted crystal growth and the crystal was constructed from a single sector of (1 0 0). It has been suggested[22,53] that the

polymer molecules in (1 0 0) sectors fold parallel to the (0 1 0) direction, i.e. parallel to the long dimension of elongated PE crystals. Now, with regard to points of dissimilarity, we note first that the arrangement of the zigzag planes differs. In PPS, Tabor *et al.*[3] determined that the zigzag planes are all parallel. In PE, the orthorhombic crystal structure has non-parallel zigzag planes[55]. Another difference is the roughness of the growth surface (or fold edges). While the PPS single crystal shows very rough crystal growth surface, the elongated PE crystal shows a curved growth surface with roughness at the molecular level.

It has also been suggested[54] that the attachment with widely separated polymer stems during crystal growth would be unlikely, not because of the limitation of crystallization kinetics, but because the space in the fold surface region will be overfilled. The types of folding of the PE single crystal have been investigated[56–58] using small angle neutron scattering, and results showed that the majority of the polymer stems in the lamellar PE single crystals exhibit adjacent re-entry along the row which is the fold direction. For PE crystallization at 70°C from xylene solution it has been reported[58] that 75% of the stems are characterized by adjacent re-entry. Based on the adjacent re-entry model of polymer stems in lamellar single crystals, Wittmann and Lotz[22] were able to determine the direction of chain folding in each sector of various PE single crystals. By using a similar decoration method, we found that when we vapour deposited PE the crystallized rods will orient to reveal the surface structure of PPS single crystals. The PE decoration rods on the crystal surface align perpendicular to the long dimension of the PPS needle crystal. This suggests according to the similar observation of Wittmann and Lotz that the PPS molecules fold along the long dimension of the needle crystals. Because the dimensions of the PPS single crystals are too small and the PPS single crystals generally show aggregation tendency during preparation of TEM specimens, we were unable to observe the spot-like diffraction pattern of the PPS single crystal along with (0 0 2) diffraction from decorating PE rods. However, we assume that the relationship of the decoration rod alignment and the topological structure of the tight fold crystal surface in the decoration of PE single crystals can also be applied to the case of PE decoration on PPS single crystals. Then we conclude the PPS molecules should fold along the long dimension of the needle crystal, i.e. the crystal growth direction. This is an area requiring further study.

We suggest that in PPS, the long dimension growth and short dimension growth are controlled by different factors resulting in the formation of needle-like crystals. If the polymer chains fold along the *b*-axis direction, the growth on the long dimension will be controlled both by nucleation rate and by crystal growth rate. Growth on the short dimension direction should be controlled predominantly by the nucleation rate. Once a nucleation site is initiated on the (1 0 0) plane, we suggest that the crystal then grows along the long dimension direction by folding polymer chains along the *b*-axis direction. The length of the short dimension is not related primarily to the crystal growth rate but rather to the nucleation rate on the existing (1 0 0) plane.

In this explanation of needle-like growth, the aspect ratio will be a function of T_c. Since the growth rate along the long dimension and nucleation rate along the short dimension have different temperature dependence, the aspect ratio will be a function of T_c. In general, the higher the T_c, the slower both growth rate and nucleation rate, but the nucleation rate is more strongly dependent on temperature than is the growth rate. Hence the aspect ratio increases as T_c rises. The aspect ratio is also a function of molecular mass. As shown in *Figure 9*, at the same degree of undercooling, the single crystal grown from the medium molecular weight film grade PPS has a higher aspect ratio than that grown from low molecular weight Ryton V-1 PPS. The long dimension is controlled by crystal growth rate, and therefore is a function of both undercooling and molecular weight. By contrast, the short dimension is controlled by nucleation rate, and is mainly a function of undercooling. Hence, under the same undercooling, we see as expected that the higher the molecular weight of the polymer, the larger the aspect ratio.

In the attempt to explain the (1 0 0) curved growth edge of PE single crystals grown at high temperature, Sadler[58] inspected the roughness of the crystal growth surface of the (1 0 0) sector. He suggested an explanation based on a molecularly rough growth surface on the curved growth surface of non-faceted single crystals. He suggested the growth faces of lamellar crystals can have an equilibrium roughness. He further suggested that it is possible to construct curvature on a macroscopic scale by the existence of a zigzag surface consisting of a sequence of 'microfacets'. By studying the effect of T_c on the PE single crystal habit, Sadler[58] also suggested that the existence of surface disorder (roughness) requires that the binding energy between the units of the crystal is comparable with kT. He found that the roughness of the growth surface is a function of kT/ε_1, the ratio of the thermal energy kT and the energy of the bonds parallel to the growth surface ε_1. When kT/ε_1 is low the growth surface resulted in faceted crystal growth with a smooth growth surface. But at high kT (typically $> \sim 0.63$ for PE) non-faceted crystal growth was observed with microscopic surface roughness on the growth surface. Thus, it is possible to explain the high anisotropy of PPS needle-like single crystals in an analogous manner involving a macroscopically very rough growth surface. It has been shown[58] that the surface roughness is a function of T_c: the higher T_c, the higher crystal anisotropy, and the higher growth surface roughness. Therefore the non-faceted crystal growth of PPS single crystals resulting in no sectorization, and the highly anisotropic characteristic with aspect ratio from 8 to 25 suggests that in PPS macroscopically rough growth surfaces can be expected.

CONCLUSIONS

A two-stage self-seeding technique has been used successfully to grow more perfect PPS single crystals from dilute solution. Two kinds of solution grown crystals are found for film grade PPS: sheaf-like aggregates and single crystals. Three types of crystals are seen in linear low molecular weight Ryton V-1: sheaf-like aggregates, big crystals and single crystals. In each starting material, the seeding conditions control the coexistence of different crystal types and determine whether isolated single crystals will be grown. PPS single crystals have a highly anisotropic needle-like crystal habit with a macroscopically smooth crystal fold surface and rough crystal

growth surface. The axial anisotropy of the needle-like single crystals is strongly dependent upon the second-stage T_c and PPS starting material.

Results of a PE decoration experiment suggest that the PPS molecule folds along the long dimension of the needle-like single crystal that is also the defined crystal growth direction. Formation of needle-like crystals, lack of sectorization, formation of macroscopically rough growth surfaces, and the molecular weight and T_c dependency of the crystal habit have been explained using Sadler's equilibrium roughness model[58].

ACKNOWLEDGEMENTS

The authors thank the J. H. and E. V. Wade Award and the Esther and Harold E. Edgerton Fund for support of this research. JSC thanks IBM for a predoctoral fellowship.

REFERENCES

1 Brady, D. J. *J. Appl. Polym. Sci.* 1976, **20**, 2541
2 Frommer, J. E., Elsenbaumer, R. L., Eckhardt, H. and Chance, R. R. *J. Polym. Sci., Polym. Lett. Edn.* 1983, **21**, 39
3 Tabor, B. J., Magre, E. P. and Boon, J. *Eur. Polym. J.* 1971, 7, 1127
4 Garbarczyk, J. *Polym. Commun.* 1986, **27**, 335
5 Lovinger, A. J., Padden, F. J. and Davis, D. D. *Polymer* 1988, **29**, 229
6 Zhang, X. and Wang, Y. *Polymer* 1989, **60**, 1867
7 Lopez, L. C. and Wilkes, G. *Polymer* 1988, **29**, 106
8 Lovinger, A. J., Davis, D. D. and Padden, F. J. *Polymer* 1985, **26**, 1595
9 Cheng, S., Wu, Z. and Wunderlich, B. *Macromolecules* 1987, **20**, 2802
10 Lopez, L. and Wilkes, G. *Polymer* 1989, **30**, 882
11 Lopez, L., Wilkes, G. and Geibel, J. *Polymer* 1989, **30**, 147
12 Padden, F. J. and Lovinger, A. J. *Bull. Am. Phys. Soc.* 1982, **27**, 259
13 Lovinger, A. J. personal communication, 1990
14 Uemura, A., Isoda, S., Tsuji, M., Ohara, M., Kawaguchi, A. and Katayama, K. *Bull. Inst. Chem. Res., Kyoto Univ.* 1986, **64**, 66
15 Uemura, A., Tsuji, M., Kawaguchi, A. and Katayama, K. *J. Mater. Sci.* 1988, **23**, 1506
16 D'Ilario, L. and Piozzi, A. *J. Mater. Sci. Lett.* 1989, **8**, 157
17 D'Ilario, L. and Piozzi, A. VIII Convegno Italiano Di Scienza Delle Macromolecole, October 1987, Associazione Italiana di Scienza e Technologia delle Macromolecole, Milan, pp. 469–472
18 Blundell, D. J. and Keller, A. *J. Macromol. Sci., Phys. B2* 1986, **2**, 301
19 Passaglia, E. and Khoury, F. *Polymer* 1984, **25**, 631
20 Markert, C. L., Blair, H. E. and Kelleher, P. G. *Proc. 7th Int. Conf. Thermal Anal.* 1982, **2**, 1362; *US Pat 3 793 256*, 1974; *US Pat 4 447 597*, 1984; *US Pat 4 424 338*, 1984
21 Blundell, D. J. and Keller, A. *J. Macromol. Sci., Phys. B2* 1968, **2**, 337
22 Wittmann, J. C. and Lotz, B. *J. Polym. Sci., Polym. Phys. Edn.* 1985, **23**, 205
23 Woodward, A. E. 'Atlas of Polymer Morphology', Hanser Publishers, Munich, 1989, IIIA.9
24 D'Ilario, L. and Piozzi, A. *Thermochim. Acta* 1989, **149**, 101
25 D'Ilario, L. and Piozzi, A. *Thermochim. Acta* 1989, **146**, 233
26 Cebe, P. and Chung, S. *Polym. Composites* 1990, **11**, 265
27 Hamada, F., Wunderlich, B., Sumida, T., Hayashi, S. and Nakajima, A. *J. Phys. Chem.* 1968, **72**, 178
28 Statton, W. O. and Geil, P. H. *J. Appl. Polym. Sci.* 1960, **32**, 2332
29 Jaffe, M. and Wunderlich, B. *Kolloid Z. Z. Polym.* 1967, **203**, 216
30 Lemstra, P. J., Kooistrom, T. and Challa, G. *J. Polym. Sci., Polym. Phys. Edn.* 1972, **10**, 823
31 Geil, P. H. *J. Polym. Sci.* 1960, **XLIV**, 449
32 Holland, V. F. and Miller, R. L. *J. Appl. Phys.* 1964, **35**, 3241
33 Holland, V. F. *Makromol. Chem.* 1964, **71**, 204
34 Sauer, J. A., Morrow, D. R. and Richardson, G. C. *J. Appl. Phys.* 1965, **36**, 3017
35 Padden Jr, F. J. and Keith, H. D. *J. Appl. Phys.* 1965, **36**, 2987
36 Niegisch, W. D. *J. Polym. Sci. B* 1966, **4**, 531
37 Utsunomiya, H., Kawasaki, N., Niinomi, M. and Takayanagi, M. *J. Polym. Sci. B* 1967, **5**, 907
38 Woodward, A. E. and Morrow, D. R. *J. Polym. Sci. A2* 1968, **6**, 1987
39 Keith, H. D., Giannoni, G. and Padden, F. J. *Biopolymer* 1979, 7, 775
40 Hachiboshi, M., Fukuda, T. and Kobayashi, S. *J. Macromol. Sci.–Phys.* 1969, **B3**, 525
41 Dreyfuss, P. and Keller, A. *J. Macromol. Sci. Phys. B4* 1970, **4**, 811
42 Kojima, M. and Magill, J. H. *Polym. Commun.* 1983, **25**, 329
43 Kojima, M., Kluge, W. and Magill, J. H. *Macromolecules* 1984, **17**, 1421
44 Lovinger, A. J. and Davis, D. D. *Macromolecules* 1986, **19**, 1861
45 Lovinger, A. J. and Davis, D. D. *Polym. Commun.* 1985, **26**, 322
46 Waddon, A. J., Hill, M. J., Keller, A. and Blundell, D. J. *J. Mater. Sci.* 1987, **22**, 1773
47 Lovinger, A. J. and Davis, D. D. *J. Appl. Phys.* 1985, **58**, 2843
48 Keith, H. D. *J. Appl. Phys.* 1964, **35**, 3115
49 Khoury, F. and Bolz, L. H. '38th Ann. Proc. Electron Microscopy Soc. Am.' (Ed. G. W. Baily), San Francisco Press, San Francisco, 1980, p. 242
50 Valenti, B. and Pedemonte, E. *Chim. Ind.* 1972, **54**, 112
51 Keith, H. D. and Padden, F. J. *J. Appl. Phys.* 1964, **35**, 1286
52 Keith, H. D. and Padden, F. J. *J. Appl. Phys.* 1964, **35**, 3115
53 Bassett, D. C., Frank, F. C. and Keller, A. *Nature* 1959, **811**, 810
54 Sadler, D. M. and Keller, A. *Macromolecules* 1977, **10**, 1128
55 Wunderlich, B. 'Macromolecular Physics', Vol. 1, Academic Press, New York, 1979, pp. 85–95
56 Stamm, M., Fischer, E. W. and Oettenmaier, M. *Faraday Discuss.* 1979, **68**, 263
57 Yoon, D. Y. and Flory, P. J. *Faraday Discuss.* 1979, **68**, 10
58 Sadler, D. M. *Polymer* 1983, **24**, 1401